

# Highly Efficient Indirect Hydration of Olefins to Alcohols Using Superacidic Polyoxometalate-Based Ionic Hybrids Catalysts

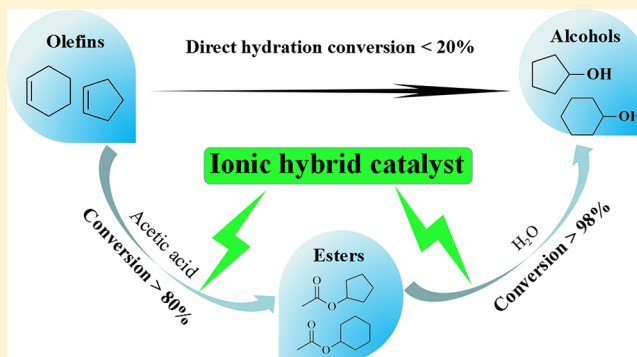
Zhi-Jun Cao,<sup>†</sup> Xin Zhao,<sup>†</sup> Fei-Qiang He,<sup>†</sup> Yan Zhou,<sup>†</sup> Kuan Huang,<sup>‡</sup> An-Min Zheng,<sup>§</sup> and Duan-Jian Tao<sup>\*,†</sup>

<sup>†</sup>College of Chemistry and Chemical Engineering, Institute of Advanced Materials, Jiangxi Normal University, Nanchang 330022, China

<sup>‡</sup>Key Laboratory of Poyang Lake Environment and Resource Utilization of Ministry of Education, School of Resources Environmental and Chemical Engineering, Nanchang University, Nanchang 330031, China

<sup>§</sup>Wuhan Center for Magnetic Resonance, State Key Laboratory of Magnetic Resonance and Atomic and Molecular Physics, Wuhan Institute of Physics and Mathematics, Chinese Academy of Sciences, Wuhan 430071, China

**ABSTRACT:** Improving the catalytic efficiency in the hydration of olefins to alcohols is an important yet challenging issue in acid catalysis. Herein, a series of novel superacidic polyoxometalate-based ionic hybrids were prepared and employed as catalysts for highly efficient indirect hydration of olefins to corresponding alcohols. Several characterization techniques such as FT-IR spectra, XRD, SEM, and <sup>31</sup>P MAS NMR spectroscopy were performed to characterize the structures of these superacid hybrids and their acid properties. The results show that the catalytic performances of ionic hybrids were closely related to their acidic strength. The superacidic ionic hybrid [BPy-SO<sub>3</sub>H-OTf]PW was found to be the best active catalyst to obtain the corresponding alcohols with good yields. The catalytic efficiency in indirect hydration process using superacidic ionic hybrid catalysts is obviously superior to that of direct hydration, which thus opens up a new way to improve the efficiency of the current hydration process.



## INTRODUCTION

Alcohols are of critical importance to both synthetic and pharmaceutical industries as reactants and industrial solvents. Typically, the addition of water to olefins is a fundamental transformation to yield alcohols. Generally, there are two ways to achieve this process: direct hydration and indirect hydration.<sup>1–4</sup> The conventional direct hydration process occurs through the treatment of alkene with water using strong acid catalysis through a carbocation intermediate.<sup>5–7</sup> For example, HZSM-5 zeolite catalysts were widely applied to accelerate the hydration of cyclohexene to cyclohexanol.<sup>7</sup> Because of the extremely poor miscibility of water and cyclohexene, the reaction rate is very low and thus the yield was <20%. Consequently, the direct hydration process suffers from many inevitable disadvantages including very low conversion and yield, large amounts of catalyst, and high energy consumption.

As an alternative, indirect hydration has captured our intensive attention because of its high conversion/selectivity and low-energy process.<sup>8,9</sup> For example, the indirect hydration route for the preparation of cyclohexanol can be described as a two-step process, which involves the first step of the esterification of cyclohexene with formic acid (or acetic acid) to form the corresponding ester and the second step of the hydrolysis of the obtained ester to produce cyclohexanol. The feasibility of this methodology had been confirmed by Steyer

and co-workers,<sup>8</sup> indicating the advantages of high reaction selectivity, low pollution and corrosion, and mild reaction conditions. Moreover, it is worth noting that the esterification of cyclohexene with carboxylate acid is the determining step in the whole indirect hydration.<sup>10</sup> That is to say, improving the rate of the first step of indirect hydration can effectively increase the yield of target product alcohol, in which the activity of catalysts employed is particularly important. However, the conventional solid acid catalyst ion-exchange resins Indion-130 and Amberlyst-15 were found to induce <50% conversions of cyclohexene in the esterification of cyclohexene and formic acid.<sup>8</sup> Thus, this poor catalytic performance still restricts the wide range of application of alcohol production from olefin by indirect hydration in industry.

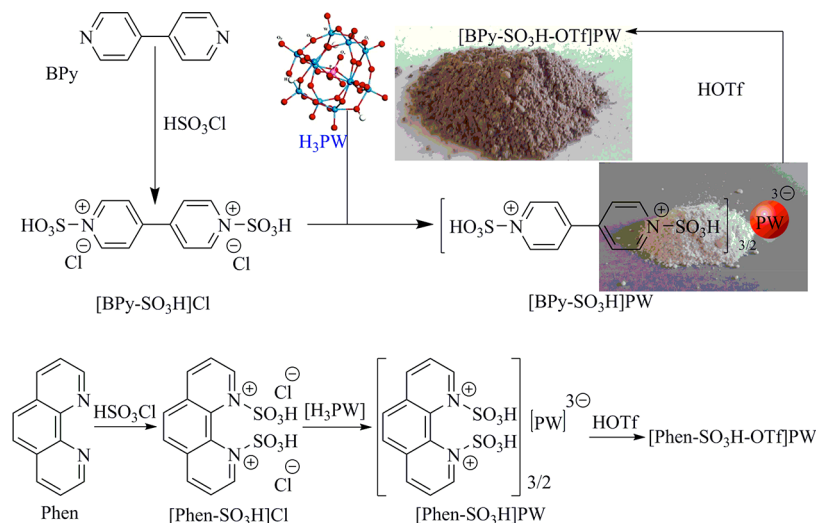
It is well-known that the esterification of olefin involves the addition of proton to alkene, which forms a carbocation-like intermediate or transition state. Then the acid strength of the acidic catalyst plays a key role in the generation of carbocation and thus determines the degree of reactivity. The catalyst with strong acidity could also accelerate the second-step hydrolysis

Received: February 2, 2018

Revised: March 17, 2018

Accepted: April 26, 2018

Published: April 26, 2018

Scheme 1. Preparation of Ionic Hybrids [BPy-SO<sub>3</sub>H-OTf]PW and [Phen-SO<sub>3</sub>H-OTf]PW

of ester to alcohol.<sup>11–13</sup> It suggests that high-yielding alcohol production by indirect hydration is closely related to the acid strength of catalyst used. Thus, exploration of novel superacidic catalysts with high activity is highly conceived and desired for the indirect hydration process. Recently, polyoxometalate-based ionic liquids (ILs) serving as solid acid materials have received considerable attention owing to their unique properties of combining ILs and heteropolyacids, including strong acidity, high thermal stability, negligible volatility, and virtually unlimited tunability.<sup>14–24</sup> Several acidic polyoxometalate-based ionic hybrids exhibited superior catalytic performance in many acid-catalyzed reactions such as esterification,<sup>15,17</sup> transesterification,<sup>21</sup> and alkylation,<sup>22</sup> demonstrating that they would show great potential application in indirect hydration of olefin to alcohol.

Herein, we prepared a series of novel superacidic polyoxometalate-based ionic hybrids by grafting polyoxometalate and sulfonic acid group on 4,4'-bipyridine and 1,10-phenanthroline as highly efficient catalysts for indirect hydration of olefin to alcohol. Acid properties of polyoxometalate-based ionic hybrids were characterized by solid-state phosphor-31 magic-angle-spinning nuclear magnetic resonance (<sup>31</sup>P MAS NMR) spectroscopy using trimethylphosphine oxide (TMPO) as a probe molecule. Fourier transform infrared (FT-IR) spectra, powder X-ray diffraction (XRD), and scanning electron microscopy (SEM) were also performed to characterize the structures of these superacid hybrids. Then their catalytic behavior in indirect hydration of alkene was investigated in detail. The reaction parameters such as catalyst loading, reaction time, temperature, and molar ratio of reactants were systematically investigated to obtain the optimum conditions.

## EXPERIMENTAL SECTION

**Materials.** 4,4'-Bipyridine (Bpy, 99%), 1,10-phenanthroline (Phen, 99%), chlorosulfonic acid (99.5%), sulfuric acid (H<sub>2</sub>SO<sub>4</sub>, 98%), trifluoromethanesulfonic acid (TfOH, 98%), phosphotungstic acid (H<sub>3</sub>PW, 99.5%), sodium carbonate (Na<sub>2</sub>CO<sub>3</sub>, 99.5%), 1-hexene (99%), cyclopentene (98%), cyclohexene (99%), formic acid (99%), acetic acid (99%), propanoic acid (99%), butyric acid (99%), pentanoic acid (99%), and hexanoic acid (99%) were purchased from Adamas Chemical Reagent

Co., Ltd. The resin Amberlyst-15 was obtained from Rohm and Haas Co., Ltd. Other materials and solvents were obtained in the highest purity grade possible and used as received.

**Synthesis of Ionic Hybrids.** The sulfonic acid-functionalized 4,4'-bipyridinium salt was prepared by referring to the literature.<sup>25</sup> The preparation procedure is as follows (Scheme 1): 4,4'-bipyridine (1.56 g) was added to a 50 mL three-necked flask containing anhydrous CH<sub>2</sub>Cl<sub>2</sub> (20 mL). Then 2.33 g of chlorosulfonic acid was added slowly into the flask at 0 °C within 20 min, stirring for 12 h under nitrogen atmosphere. After reaction, solid white powder was obtained from filtering, washing with pure CH<sub>2</sub>Cl<sub>2</sub> (3 × 20 mL), and drying at 70 °C. The sample was denoted as [BPy-SO<sub>3</sub>H]Cl.

A polyoxometalate [BPy-SO<sub>3</sub>H]PW was synthesized according to the previous method in a precipitation process.<sup>26</sup> An aqueous solution (30 mL) of H<sub>3</sub>PW (5.76 g) was added slowly to 25 mL of aqueous solution of [BPy-SO<sub>3</sub>H]Cl (1.16 g), followed by stirring at room temperature for 24 h. The product [BPy-SO<sub>3</sub>H]PW was obtained from filtering, washing with water, and drying at 80 °C under vacuum.

Polyoxometalate-based ionic hybrid [BPy-SO<sub>3</sub>H-OTf]PW was prepared by the further treatment of [BPy-SO<sub>3</sub>H]PW with modification of TfOH, which results in grafting of a strong electron-withdrawing group of SO<sub>2</sub>CF<sub>3</sub> onto the network of polyoxometalate-based ionic salt [BPy-SO<sub>3</sub>H]PW.<sup>27,28</sup> In a typical run, 1 g of [BPy-SO<sub>3</sub>H]PW was added into a flask containing 20 mL of toluene, followed by addition of 5 mL of TfOH. Then the reaction mixture was stirred for 24 h at 105 °C. After the reaction finished, the mixture was filtered, washed with a large amount of CH<sub>2</sub>Cl<sub>2</sub>, and dried in vacuum oven at 80 °C to obtain the product [BPy-SO<sub>3</sub>H-OTf]PW.

The synthesis procedure of the other three samples, [Phen-SO<sub>3</sub>H]Cl, [Phen-SO<sub>3</sub>H]PW, and [Phen-SO<sub>3</sub>H-OTf]PW (Scheme 1), was similar to that described in the preparation of [BPy-SO<sub>3</sub>H]Cl, [BPy-SO<sub>3</sub>H]PW, and [BPy-SO<sub>3</sub>H-OTf]PW, respectively.

**Characterization of Ionic Hybrids.** The C, N, H, and S elemental analysis of ionic hybrids was carried out on Elementar Vario El III. Fourier transform infrared spectroscopy (FT-IR) spectra were recorded on NEXUS870 FT-IR spectrometer. Powder X-ray diffraction (XRD) patterns were recorded on a Rigaku RINT-2200 X-ray diffractometer using

Cu  $K\alpha$  radiation (40 kV, 20 mA). The field-emission SEM measurements were performed using a HITACHI SU8020 cold field-emission instrument.

NMR experiments were performed on a Bruker Ascend-500 spectrometer at a resonance frequency of 202.63 MHz for  $^{31}\text{P}$ , with a 4 mm triple-resonance MAS probe at a spinning rate of 10 kHz.  $^{31}\text{P}$  MAS NMR spectra with high-power proton decoupling were recorded using a  $\pi/2$  pulse length of 4.1  $\mu\text{s}$  and a recycle delay of 30 s. The chemical shift of  $^{31}\text{P}$  was referenced to 1 M aqueous  $\text{H}_3\text{PO}_4$ . According to the method reported in the previous references,<sup>13</sup> the solid  $^{31}\text{P}$  NMR spectra over four samples of polyoxometalate-based ionic hybrids were performed as follows: prior to the adsorption of probe molecules, the samples were placed in glass tubes and connected to a vacuum line for dehydration. The temperature was gradually increased at a rate of 1  $^\circ\text{C min}^{-1}$ , and the samples were kept at a final temperature of 100  $^\circ\text{C}$  and a pressure below  $10^{-3}$  Pa over a period of 10 h and then cooled. After the samples cooled to room temperature, a known amount of trimethylphosphine oxide (TMPO) adsorbate dissolved in anhydrous  $\text{CH}_2\text{Cl}_2$  was first added into a vessel containing the dehydrated sample in a  $\text{N}_2$  glovebox, followed by removal of the  $\text{CH}_2\text{Cl}_2$  solvent by evacuation at room temperature. Finally, the sample tubes were flame-sealed. Prior to NMR experiments, the sealed samples were transferred into  $\text{ZrO}_2$  rotors with a Kel-F end-cap under a dry nitrogen atmosphere in a glovebox.

#### General Reaction Procedures for Indirect Hydration.

First, the polyoxometalate-based ionic hybrids were employed as catalysts for the esterification of cyclopentene with acetic acid. In a typical run, cyclopentene (10 mmol), acetic acid (30 mmol), and [BPy- $\text{SO}_3\text{H-OTf}$ ]PW catalyst (20 wt %, base on the mass of acetic acid and cyclopentene) were added into a 25 mL round-bottomed flask equipped with a magnetic stirrer. The reaction mixture was stirred at 80  $^\circ\text{C}$  for 15 h. After the reaction, the products were identified by gas chromatography–mass spectrometry (GC-MS) (Thermo Trace 1300 GC-ISQ) and quantified by a GC-FID (Agilent 7890B) equipped with a capillary column HP-5 (methyl polysiloxane, 30 m  $\times$  0.32 mm  $\times$  1  $\mu\text{m}$ ). Trimethylbenzene was used as internal standard to quantify the products. The detailed analysis conditions were described as follows: the temperatures of injector and detector were all 200  $^\circ\text{C}$ . The column temperature was increased from 50 to 120  $^\circ\text{C}$  at 10  $^\circ\text{C min}^{-1}$ , holding at 120  $^\circ\text{C}$  for 10 min.

After the first step of esterification, the reaction mixture was heated to 120  $^\circ\text{C}$  to directly distill excess reactant acetic acid, and then the residue mainly contained cyclopentyl acetate and catalyst [BPy- $\text{SO}_3\text{H-OTf}$ ]PW. Subsequently, the deionized water (2.24 g) was added into the flask. The second step of hydrolysis of cyclopentyl acetate was performed at 80  $^\circ\text{C}$  for 2.5 h to obtain the corresponding cyclopentyl alcohol. After the reaction finished, the liquid phase was taken from the reactor and also analyzed by GC-MS and GC, while the solid catalyst was easily separated by filtration and was recycled by drying under vacuum at 90  $^\circ\text{C}$  for 12 h.

## RESULTS AND DISCUSSION

**Acidic Properties of Ionic Hybrids.** It is well-known that the acidic properties of solid acid catalyst including the acid type (Brønsted vs Lewis acidity), strength, and concentration play a significant role in affecting the activity and selectivity during catalytic reactions. As verified by the previous literature, solid-state  $^{31}\text{P}$  MAS with TMPO probe is highly sensitive in terms of characterization of Brønsted acid strengths in acids, in

which acid strength can be measured through  $^{31}\text{P}$  chemical shift, and  $^{31}\text{P}$  chemical shift threshold value of superacid was found to be 86 ppm.<sup>29–34</sup> Such method has been widely used to study the acidity characterization of various solid acids, including zeolites,<sup>29,30</sup> heteropolyacids,<sup>31,32</sup> and sulfated mesoporous metal oxides.<sup>33,34</sup> Figure 1 shows the  $^{31}\text{P}$  MAS NMR

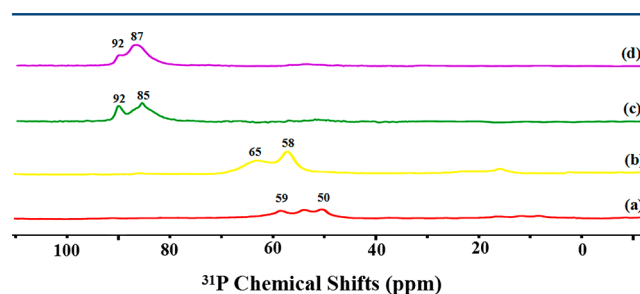


**Figure 1.** Solid-state  $^{31}\text{P}$  MAS NMR of adsorbed TMPO on (a) [BPy- $\text{SO}_3\text{H}$ ]PW, (b) [Phen- $\text{SO}_3\text{H}$ ]PW, (c) [BPy- $\text{SO}_3\text{H-OTf}$ ]PW, and (d) [Phen- $\text{SO}_3\text{H-OTf}$ ]PW.

spectrum of TMPO adsorbed on four samples of polyoxometalate-based ionic hybrids. It is seen that [BPy- $\text{SO}_3\text{H}$ ]PW showed  $^{31}\text{P}$  resonance peaks spanning from ca. 50 to 60 ppm, while [BPy- $\text{SO}_3\text{H-OTf}$ ]PW displayed two characteristic resonances with  $^{31}\text{P}$  chemical shift of 85 and 92 ppm. For [Phen- $\text{SO}_3\text{H-OTf}$ ]PW, two characteristic resonance  $^{31}\text{P}$  peaks with chemical shift at 87 and 92 ppm were also observed. However, [Phen- $\text{SO}_3\text{H}$ ]PW resulted the  $^{31}\text{P}$  resonance peaks of 58 and 65 ppm. These results demonstrated that  $^{31}\text{P}$  chemical shift values were  $>86$  ppm, indicating the presence of Brønsted superacidity in [BPy- $\text{SO}_3\text{H-OTf}$ ]PW and [Phen- $\text{SO}_3\text{H-OTf}$ ]PW. These two ionic hybrids are considered to be Brønsted solid superacids. After the treatment by using superacid of  $\text{HSO}_3\text{CF}_3$ , the strong electron-withdrawing group  $\text{SO}_2\text{CF}_3$  was grafted onto the network of [BPy- $\text{SO}_3\text{H-OTf}$ ]PW and [Phen- $\text{SO}_3\text{H-OTf}$ ]PW, respectively. Consequently, the Brønsted acidic strength of [BPy- $\text{SO}_3\text{H-OTf}$ ]PW and [Phen- $\text{SO}_3\text{H-OTf}$ ]PW had been remarkably enhanced.

Table 1 presents the sulfur content and acid concentration of four ionic hybrids samples. It is found that [BPy- $\text{SO}_3\text{H-}$

**Table 1.** Acidic Properties of Ionic Hybrids Catalysts

entry	catalyst	acid sites <sup>a</sup> (mmol/g)	S content <sup>b</sup> (mmol/g)
1	[BPy- $\text{SO}_3\text{H-OTf}$ ]PW	1.57	1.96
2	[Phen- $\text{SO}_3\text{H-OTf}$ ]PW	1.35	1.51
3	[BPy- $\text{SO}_3\text{H}$ ]PW	1.22	0.94
4	[Phen- $\text{SO}_3\text{H}$ ]PW	1.18	0.93

<sup>a</sup>Measured by acid–base titration. <sup>b</sup>Measured by elemental analysis.

OTf]PW and [Phen- $\text{SO}_3\text{H-OTf}$ ]PW had high concentrations of sulfonic groups (entries 1 and 2). In contrast, [BPy- $\text{SO}_3\text{H}$ ]PW and [Phen- $\text{SO}_3\text{H}$ ]PW showed relatively low concentrations of sulfonic groups (entries 3 and 4). These results indicate that the introduction of the superacid group  $\text{SO}_2\text{CF}_3$  to [BPy- $\text{SO}_3\text{H-OTf}$ ]PW and [Phen- $\text{SO}_3\text{H-OTf}$ ]PW could effectively improve their sulfur content and acid concentration.

**Characterization of Superacidic Ionic Hybrids.** Figure 2a illustrates the FT-IR spectra of [BPy- $\text{SO}_3\text{H-OTf}$ ]PW and [BPy- $\text{SO}_3\text{H}$ ]PW as well as the precursor [BPy- $\text{SO}_3\text{H}$ ]Cl for

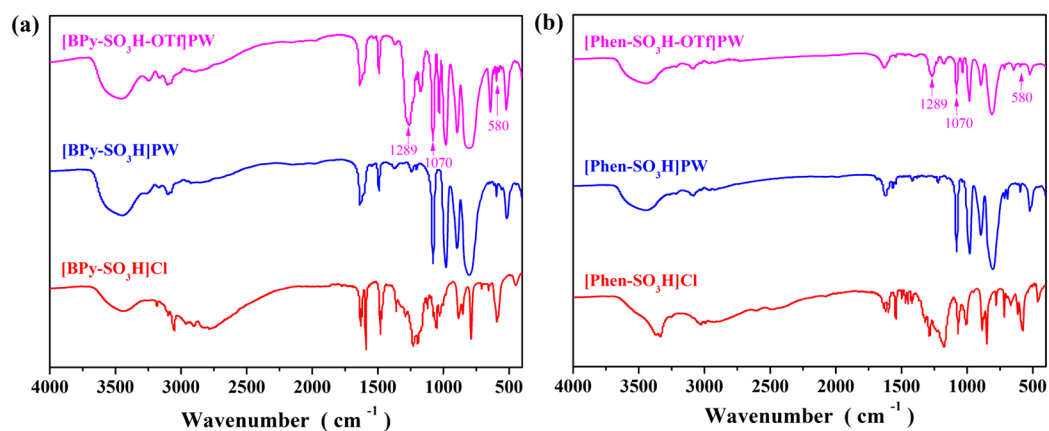


Figure 2. (a) FT-IR spectra of [BPy-SO<sub>3</sub>H]Cl, [BPy-SO<sub>3</sub>H]PW, and [BPy-SO<sub>3</sub>H-OTf]PW; (b) FT-IR spectra of [Phen-SO<sub>3</sub>H]Cl, [Phen-SO<sub>3</sub>H]PW, and [Phen-SO<sub>3</sub>H-OTf]PW.

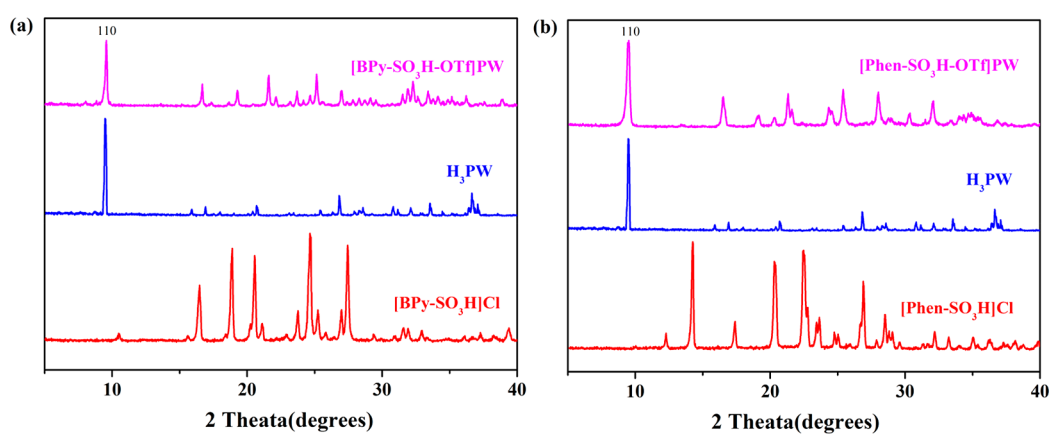


Figure 3. (a) XRD patterns of [BPy-SO<sub>3</sub>H]Cl, H<sub>3</sub>PW, and [BPy-SO<sub>3</sub>H-OTf]PW; (b) XRD patterns of [Phen-SO<sub>3</sub>H]Cl, [Phen-SO<sub>3</sub>H]PW, and [Phen-SO<sub>3</sub>H-OTf]PW.

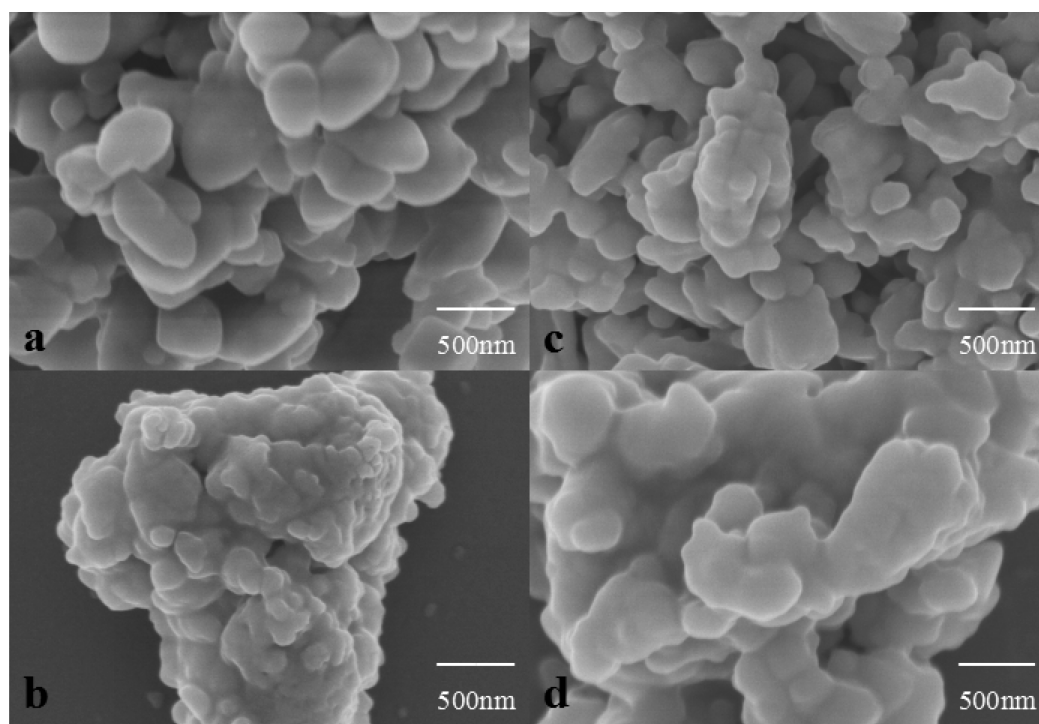
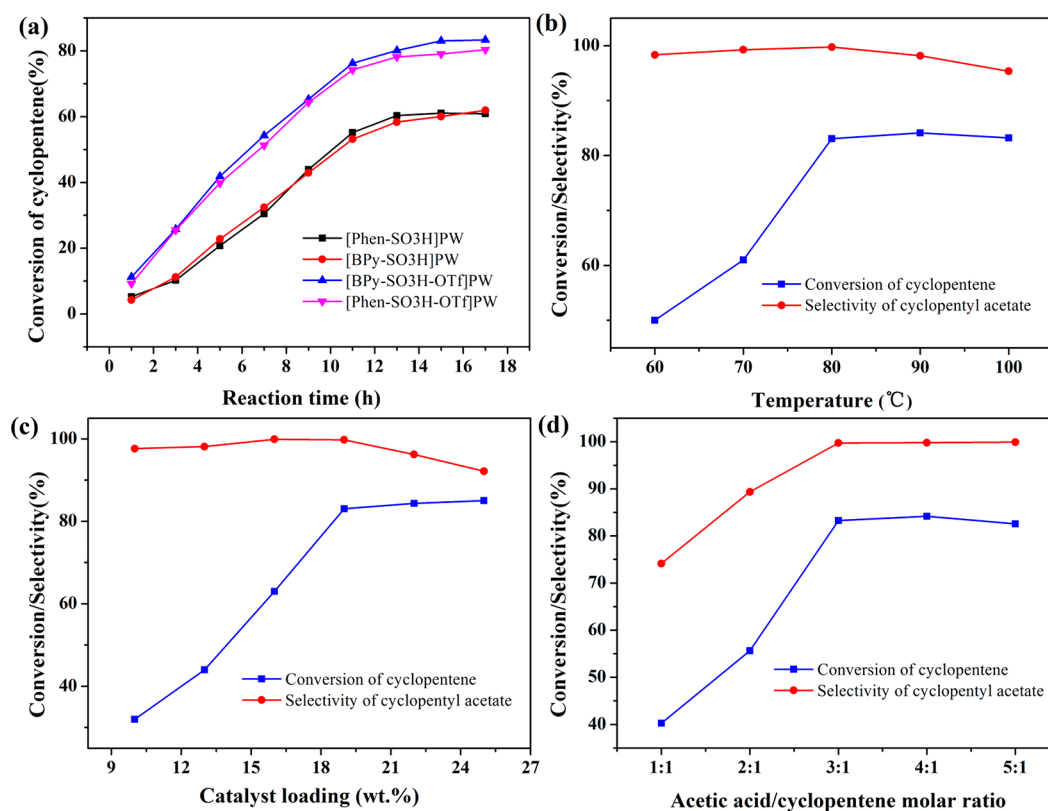


Figure 4. SEM images of (a) [BPy-SO<sub>3</sub>H]PW, (b) [BPy-SO<sub>3</sub>H-OTf]PW, (c) [Phen-SO<sub>3</sub>H]PW, and (d) [Phen-SO<sub>3</sub>H-OTf]PW.



**Figure 5.** (a) Esterification of cyclopentene catalyzed by four polyoxometalate ionic hybrids. Effect of (b) reaction temperature, (c) catalyst loading, and (d) acetic acid/cyclopentene molar ratio on the reaction using [BPy-SO<sub>3</sub>H-OTf]PW as catalyst.

comparison. It is indicated that the FT-IR spectra of [BPy-SO<sub>3</sub>H]Cl, [BPy-SO<sub>3</sub>H-OTf]PW, and [BPy-SO<sub>3</sub>H]PW had the characteristic S—O and S=O vibrations at around 580 and 1070 cm<sup>-1</sup>, respectively, indicating the existence of —SO<sub>3</sub>H group. Moreover, for [BPy-SO<sub>3</sub>H]PW and [BPy-SO<sub>3</sub>H-OTf]PW, three characteristic peaks were found at 984, 889, and 806 cm<sup>-1</sup>, which can be attributed to the stretching vibrations of W—O, W—O—W (corner-sharing), and W—O—W (edge-sharing), respectively, demonstrating that these two ionic hybrids exhibited the Keggin-type structure.<sup>35,36</sup> In addition, a new peak (1289 cm<sup>-1</sup>) assigned to C—F bond can be observed, confirming the successful graft of SO<sub>2</sub>CF<sub>3</sub> group onto [BPy-SO<sub>3</sub>H-OTf]PW, which is in good agreement with elemental analysis results.<sup>37–39</sup> It is also seen from Figure 2b that similar trends were found in the comparison of the FT-IR spectra of the other three samples, [Phen-SO<sub>3</sub>H]Cl, [Phen-SO<sub>3</sub>H]PW, and [Phen-SO<sub>3</sub>H-OTf]PW.

Figure 3 shows XRD patterns of the polyoxometalate-based ionic hybrids and their precursors [BPy-SO<sub>3</sub>H]Cl, [Phen-SO<sub>3</sub>H]Cl, and H<sub>3</sub>PW. It can be seen that [BPy-SO<sub>3</sub>H]Cl exhibited diffraction lines of a highly crystalline structure.<sup>40</sup> H<sub>3</sub>PW also showed typically sharp diffraction peaks for a HPA crystal, indicating the existence of Keggin anions (PDF no. 50-0304).<sup>29</sup> Moreover, the XRD pattern of resultant [BPy-SO<sub>3</sub>H-OTf]PW sample had the characteristic peaks at diffraction angles of 17.51, 19.77, 21.45, 24.20, 25.63, and 27.55, which was also present in the powder XRD patterns of [BPy-SO<sub>3</sub>H]Cl. The peak at 10.25° assigned to the [110] phase for parent H<sub>3</sub>PW can be also observed in the XRD pattern of [BPy-SO<sub>3</sub>H-OTf]PW, indicating the formation of HPA crystal structure in [BPy-SO<sub>3</sub>H-OTf]PW and thus showing the successful preparation of polyoxometalate-based ionic hybrids.

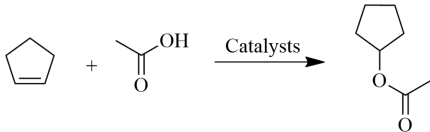
SEM was performed to characterize the morphology of polyoxometalate-based ionic hybrids as shown in Figure 4. It was seen that the parents [BPy-SO<sub>3</sub>H]PW and [Phen-SO<sub>3</sub>H]PW were microsized disordered particles in the size of 300–500 nm (Figure 4a and c).<sup>41</sup> However, compared with the precursors, the formed [BPy-SO<sub>3</sub>H-OTf]PW and [Phen-SO<sub>3</sub>H-OTf]PW particles had stacked and their sizes increased slightly (Figure 4b and d), implying the introduction of SO<sub>2</sub>CF<sub>3</sub> group into [BPy-SO<sub>3</sub>H-OTf]PW and [Phen-SO<sub>3</sub>H-OTf]PW. In addition, it can be seen from Scheme 1 that the sample [BPy-SO<sub>3</sub>H-OTf]PW turned brown in comparison to the precursor [BPy-SO<sub>3</sub>H]PW, further confirming the successful preparation of the superacid polyoxometalate-based ionic hybrid [BPy-SO<sub>3</sub>H-OTf]PW.

**First Step of Esterification Reaction.** The first step of the esterification of cyclopentene with acetic acid was performed to obtain cyclopentyl acetate using superacid polyoxometalate ionic hybrids as catalysts. As seen from Figure 5a, it was obviously indicated that the catalyst polyoxometalate-based ionic hybrids displayed various catalytic activities. Compared with the other three ionic hybrids, [BPy-SO<sub>3</sub>H-OTf]PW was demonstrated to be the best active catalyst to obtain an 85% yield of cyclopentyl acetate. Moreover, combined with the acidic strength sequence from Figure 1, it is worth noting that the catalytic performances of such ionic hybrids were closely related to their acidic strength. The esterification of olefin involves the addition of proton to alkene, in which the acid strength of the acidic catalyst plays a key role in the generation of carbocation intermediate and thus determines the degree of reactivity.<sup>13</sup> Consequently, the ionic hybrid owning superacidic strength can induce a relatively high yield of cyclopentyl acetate. In addition, to obtain the optimum conditions, reaction

parameters such as reaction time, temperature, catalyst amount, and initial molar ratio of reactants were studied in detail (Figure 5b–d). The optimized conditions thus can be set as follows: [BPy-SO<sub>3</sub>H-OTf]PW catalyst dosage of 20 wt %, acetic acid/cyclopentene molar ratio of 3:1, temperature of 80 °C, and reaction time of 15 h.

Furthermore, we employed several traditional acid catalysts and the precursors as reference catalysts to support the outstanding catalytic property of polyoxometalate ionic hybrids catalysts in the esterification of cyclopentene. The results are listed in Table 2. It is indicated that the esterification reaction

**Table 2. Results of Esterification of Cyclopentene with Acetic Acid Catalyzed by Different Catalysts<sup>a</sup>**



entry	catalyst	conversion <sup>a</sup> (%)	selectivity (%)
1	blank	0	0
2	[BPy-SO <sub>3</sub> H]Cl	40	>99
3	[Phen-SO <sub>3</sub> H]Cl	39	>99
4	[BPy-SO <sub>3</sub> H]PW	61	>99
5	[Phen-SO <sub>3</sub> H]PW	58	>99
6	[BPy-SO <sub>3</sub> H-OTf]PW	85	>99
7	[Phen-SO <sub>3</sub> H-OTf]PW	81	>99
8 <sup>b</sup>	H <sub>2</sub> SO <sub>4</sub>	65	93
9 <sup>b</sup>	PTSA	71	97
10 <sup>b</sup>	Amberlyst-15	41	>99

<sup>a</sup>Reaction conditions: molar ratio of acetate acid to cyclopentene (3:1), catalyst dosage (20 wt %), reaction temperature (80 °C), reaction time (15 h). <sup>b</sup>The same amount of acidic sites as that of [BPy-SO<sub>3</sub>H-OTf]PW.

hardly occurred without any catalysts, while the raw materials [BPy-SO<sub>3</sub>H]Cl and [Phen-SO<sub>3</sub>H]Cl showed low cyclopentene conversions of 40% and 39%, respectively (Table 2, entries 1–3). Meanwhile, liquid acid catalysts H<sub>2</sub>SO<sub>4</sub> and *p*-toluenesulfonic acid (PTSA) induced considerable conversions of cyclopentene comparable to that of [BPy-SO<sub>3</sub>H-OTf]PW, but their selectivities of cyclopentyl acetate were slightly low (Table 2, entries 8 and 9). The solid acid catalyst Amberlyst-15 resin also displayed very poor catalytic performance under identical conditions (Table 2, entry 10). Thus, it is validated from the comparison of catalytic performance that [BPy-SO<sub>3</sub>H-OTf]PW is considered to be a promising heterogeneous superacid catalyst with high activity and selectivity for the esterification of cyclopentene with acetic acid.

To explore the diversity of [BPy-SO<sub>3</sub>H-OTf]PW catalyst, the esterifications of other cyclic and linear olefins with various carboxylate acids were also studied. The results are listed in Table 3. It can be seen that the esterifications of cyclic olefins (cyclopentene and cyclohexene) with various carboxylate acids could approach the corresponding esters with good conversions and selectivities. However, the esterification of hexene with carboxylate acid would probably undergo the formation of a long-chain carbocation intermediate and easily lead to chain isomerization, resulting in relatively low conversions and selectivities of 2-hexyl ester.

**Second Step of Hydrolysis Reaction.** The second step of hydrolysis of the formed ester was subsequently performed to

obtain the target alcohol. Figure 6a shows the effect of reaction time on the hydrolysis of cyclopentyl acetate using [BPy-SO<sub>3</sub>H-OTf]PW as catalyst. It is indicated that prolonging reaction time could improve the yield of cyclopentanol, and when the reaction time reached 2.5 h, cyclopentyl acetate was completely hydrolyzed to generate cyclopentanol. Moreover, the effect of H<sub>2</sub>O amount on the hydrolysis of cyclopentyl acetate was also studied (Figure 6b). It is illustrated that, as the H<sub>2</sub>O/cyclopentyl acetate molar ratio increased varying from 1:1 to 20:1, the hydrolysis rate increased and the yield of cyclopentanol improved efficiently. However, when the molar ratio was >15:1, the yield of cyclopentanol did not substantially increase; thereby, the optimal molar ratio of H<sub>2</sub>O/cyclopentyl acetate is preferred to be 15:1. Furthermore, the hydrolysis of other esters cyclohexyl acetate and 2-hexyl acetate were also conducted under identical conditions. [BPy-SO<sub>3</sub>H-OTf]PW could completely hydrolyze cyclohexyl acetate and 2-hexyl acetate to produce cyclohexanol and 2-hexenol, respectively (seen in Table 4). Consequently, [BPy-SO<sub>3</sub>H-OTf]PW also can be employed as an efficient catalyst in the second step of the hydrolysis reaction for indirect hydration of olefins to alcohols.

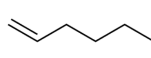
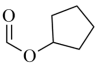
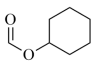
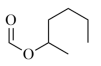
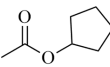
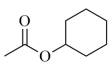
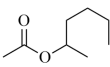
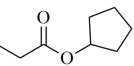
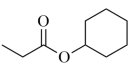
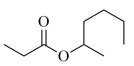
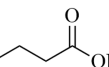
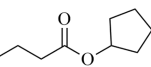
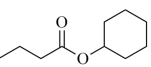
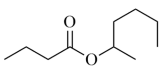
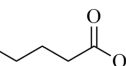
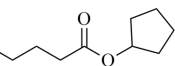
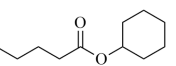
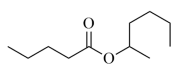
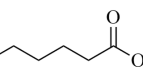
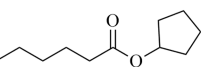
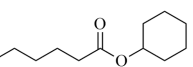
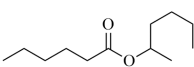
**Comparison of Indirect Hydration and Direct Hydration.** Finally, we performed the direct hydration experiments of olefins with water using [BPy-SO<sub>3</sub>H-OTf]PW as catalyst, and then the results for comparison of indirect hydration and direct hydration process are listed in Table 4. It can be seen that the yields of cyclopentanol, cyclohexanol, and hexanol with direct hydration were only 8%, 7%, and 2%, respectively, significantly lower than the corresponding yields with indirect hydration. The results demonstrate that the indirect hydration of olefins using superacidic ionic hybrid [BPy-SO<sub>3</sub>H-OTf]PW is a promising methodology for the production of alcohols. Moreover, the large-scale experiment for the indirect hydration of cyclopentene was also studied. It was indicated that the yield of cyclopentanol had not been decreased obviously, showing its great potential in an industrial scale.

**Recycling Test.** The reusability of the ionic hybrid [BPy-SO<sub>3</sub>H-OTf]PW in the preparation of cyclopentanol by indirect hydration was investigated. The data obtained in five consecutive runs are shown in Figure 7. It is indicated that no obvious decrease in the yield of cyclopentanol was observed during these five successive recycles. Moreover, hot filtration tests were taken into consideration to check the heterogeneity nature of the [BPy-SO<sub>3</sub>H-OTf]PW catalyst, and the results are shown in Figure 8. After the removal of the [BPy-SO<sub>3</sub>H-OTf]PW catalyst, it is expected that no reaction proceeded, demonstrating that the indirect hydration reaction was intrinsically heterogeneous and the catalyst would not lose acidic active species. In addition, compared with the fresh [BPy-SO<sub>3</sub>H-OTf]PW, the FT-IR spectra characteristic bands also appeared in the reused [BPy-SO<sub>3</sub>H-OTf]PW (Figure 9). These results demonstrate that the ionic hybrid [BPy-SO<sub>3</sub>H-OTf]PW is stable enough to use in the indirect hydration of cyclopentanol for several runs. The slight decrease in the activity is because of the slight mass loss of [BPy-SO<sub>3</sub>H-OTf]PW resulting from the transferring of samples.

## CONCLUSIONS

A series of novel superacidic polyoxometalate-based ionic hybrids were designed, prepared, and employed as catalysts for highly efficient indirect hydration of olefins to corresponding alcohols. Combined characterization results of FT-IR spectra,

Table 3. Esterifications of Various Carboxylate Acids with Different Olefins over [BPy-SO<sub>3</sub>H-OTf]PW Catalyst<sup>a</sup>

Entry	Substrates			
1				
	Conversion (%)	86	74	58
	Selectivity (%)	>99	>99	72
2				
	Conversion (%)	83	84	63
	Selectivity (%)	>99	>99	69
3				
	Conversion (%)	77	84	62
	Selectivity (%)	>99	>99	70
4				
	Conversion (%)	83	83	79
	Selectivity (%)	>99	>99	65
5				
	Conversion (%)	85	86	75
	Selectivity (%)	>99	>99	63
6				
	Conversion (%)	87	87	78
	Selectivity (%)	>99	>99	64

<sup>a</sup>Reaction conditions: molar ratio of acetate acid to olefins (3:1), catalyst dosage (20 wt %), reaction temperature (80 °C), reaction time (15 h).

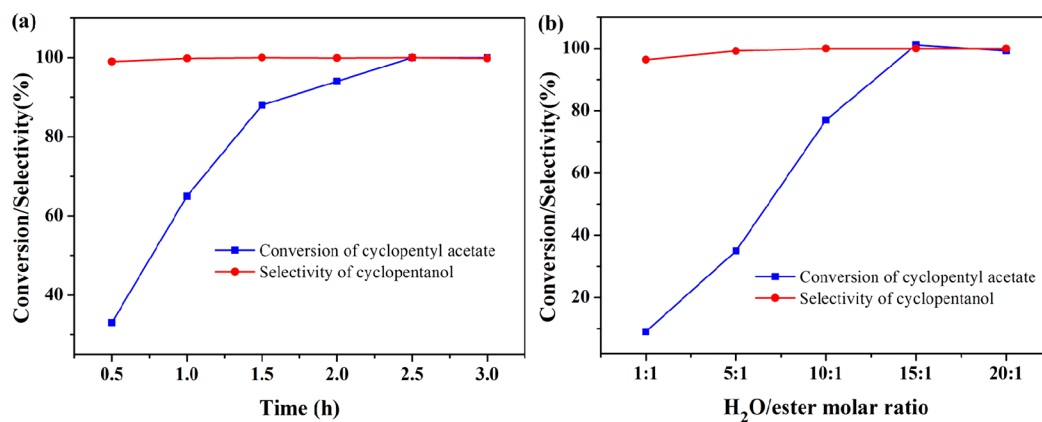
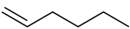


Figure 6. Effect of (a) reaction time and (b) H<sub>2</sub>O amount on the hydrolysis of cyclopentyl acetate over [BPy-SO<sub>3</sub>H-OTf]PW catalyst.

Table 4. Comparison of Indirect Hydration and Direct Hydration for the Production of Alcohols

Raw material	Product	Yield (%)	
		Indirect hydration	Direct hydration <sup>a</sup>
		83 (85 <sup>b</sup> , 98 <sup>c</sup> , 81 <sup>d</sup> )	8
		84 (86 <sup>b</sup> , 98 <sup>c</sup> )	7
		41 (43 <sup>b</sup> , 96 <sup>c</sup> )	2

<sup>a</sup>Reaction conditions: molar ratio of water to olefins (15:1), catalyst dosage (20 wt %), reaction temperature (80 °C), reaction time (17.5 h). <sup>b</sup>Yield for the first step of esterification in indirect hydration. <sup>c</sup>Yield for the second step of hydrolysis in indirect hydration. <sup>d</sup>Yield from a large-scale experiment (cyclopentene 1 mol, acetic acid 3 mol).

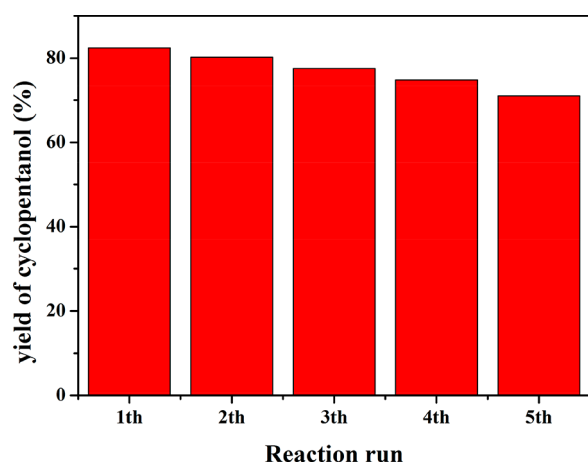
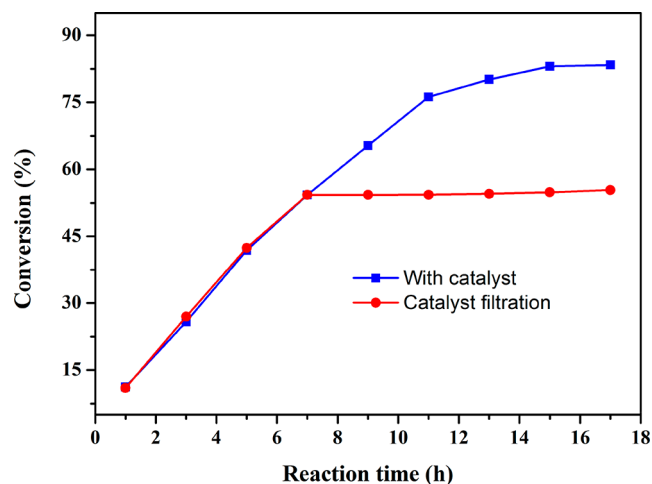
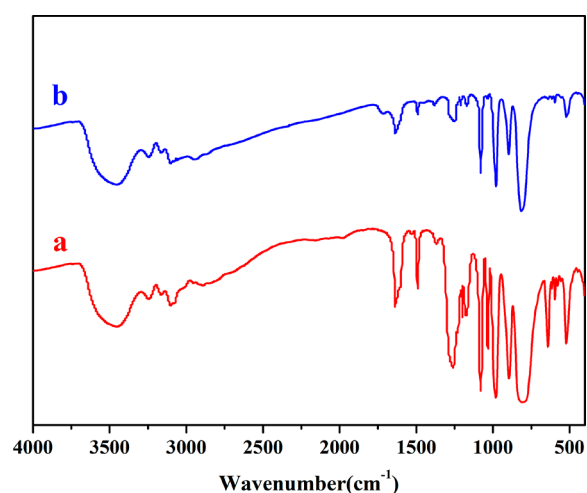
Figure 7. Recycling test of the [BPy-SO<sub>3</sub>H-OTf]PW catalyst.

Figure 8. Test of hot filtration experiment.

XRD, SEM, and <sup>31</sup>P MAS NMR spectroscopy confirmed the structures of these superacid hybrids and their Brønsted

Figure 9. FT-IR spectra of (a) fresh and (b) recycled [BPy-SO<sub>3</sub>H-OTf]PW.

superacidity. It was also found that the catalytic performance of ionic hybrids depends on their acidic strength. The super strong acidity enables ionic hybrid [BPy-SO<sub>3</sub>H-OTf]PW to have the best catalytic activities with good yields of corresponding alcohols. In addition, the catalytic efficiency in indirect hydration using superacidic ionic hybrid catalysts is significantly higher than that of direct hydration, thus showing that the indirect hydration of olefins is a promising methodology for the production of alcohols. Further exploring the indirect hydration using superacidic ionic hybrids in a large scale is underway in our laboratory.

## AUTHOR INFORMATION

### Corresponding Author

\*E-mail: [djtao@jxnu.edu.cn](mailto:djtao@jxnu.edu.cn). Tel.: +086-0791-88120380.

### ORCID

Kuan Huang: 0000-0003-1905-3017

An-Min Zheng: 0000-0001-7115-6510

Duan-Jian Tao: 0000-0002-8835-0341

## Notes

The authors declare no competing financial interest.

## ACKNOWLEDGMENTS

We thank the National Natural Science Foundations of China (nos. 21566011 and 31570560), the Jiangxi Province Sponsored Programs for Distinguished Young Scholars (no. 20162BCB23026), and the Science & Technology Programs of Jiangxi Province Department of Education (no. GJJ160272) for financial support.

## REFERENCES

- (1) Misono, M.; Inui, T. New catalytic technologies in Japan. *Catal. Today* **1999**, *51*, 369–375.
- (2) Nuntasri, D.; Wu, P.; Tatsumi, T. High selectivity of MCM-22 for cyclopentanol formation in liquid-phase cyclopentene hydration. *J. Catal.* **2003**, *213*, 272–280.
- (3) Ahamed Imam, R.; Freund, H.; Guit, R. P. M.; Fellay, C.; Meier, R. J.; Sundmacher, K. Evaluation of different process concepts for the indirect hydration of cyclohexene to cyclohexanol. *Org. Process Res. Dev.* **2013**, *17*, 343–358.
- (4) Chen, B. C.; Yu, B. Y.; Lin, Y. L.; Huang, H. P.; Chien, I. L. Reactive-distillation process for direct hydration of cyclohexene to produce cyclohexanol. *Ind. Eng. Chem. Res.* **2014**, *53*, 7079–7086.
- (5) Zheng, H.; Lin, M.; Qiu, T.; Shen, Y.; Tian, H.; Zhao, S. Simulation study of direct hydration of cyclohexene to cyclohexanol using isophorone as cosolvent. *Chem. Eng. Res. Des.* **2017**, *117*, 346–354.
- (6) Li, J.; Yang, L.; Li, F.; Xue, W.; Wang, Y. Hydration of cyclohexene to cyclohexanol over SO<sub>3</sub>H-functionalized imidazole ionic liquids. *React. Kinet., Mech. Catal.* **2015**, *114*, 173–183.
- (7) Wang, S.; Li, C.; Wen, Y.; Wei, H.; Li, B.; Wang, X. Microparticle HZSM-5 zeolite as highly active catalyst for the hydration of cyclohexene to cyclohexanol. *Res. Chem. Intermed.* **2016**, *42*, 8131–8142.
- (8) Steyer, F.; Freund, H.; Sundmacher, K. A novel reactive distillation process for the indirect hydration of cyclohexene to cyclohexanol using a reactive entrainer. *Ind. Eng. Chem. Res.* **2008**, *47*, 9581–9587.
- (9) Katariya, A.; Freund, H.; Sundmacher, K. Two-step reactive distillation process for cyclohexanol production from cyclohexene. *Ind. Eng. Chem. Res.* **2009**, *48*, 9534–9545.
- (10) Yao, B.; Wang, Z.; Xiao, T.; Cao, F.; Edwards, P. P.; Ma, W. Thermodynamic analysis of synthesis of cyclopentanol from cyclopentene and comparison with experimental data. *Appl. Petrochem. Res.* **2015**, *5*, 135–142.
- (11) Haw, J. F. Zeolite acid strength and reaction mechanisms in catalysis. *Phys. Chem. Chem. Phys.* **2002**, *4*, 5431–5441.
- (12) Tao, D. J.; Dong, Y.; Cao, Z. J.; Chen, F. F.; Chen, X. S.; Huang, K. Tuning the acidity of sulfonic functionalized ionic liquids for highly efficient and selective synthesis of terpene esters. *J. Ind. Eng. Chem.* **2016**, *41*, 122–129.
- (13) Zheng, A.; Li, S.; Liu, S. B.; Deng, F. Acidic properties and structure-activity correlations of solid acid catalysts revealed by solid-state NMR spectroscopy. *Acc. Chem. Res.* **2016**, *49*, 655–663.
- (14) Cai, X.; Wang, Q.; Liu, Y.; Xie, J.; Long, Z.; Zhou, Y.; Wang, J. Hybrid of polyoxometalate-based ionic salt and n-doped carbon toward reductant-free aerobic hydroxylation of benzene to phenol. *ACS Sustainable Chem. Eng.* **2016**, *4*, 4986–4996.
- (15) Wu, N.; Li, B.; Ma, W.; Han, C. Synthesis of lacunary polyoxometalate encapsulated into hexagonal mesoporous silica and their catalytic performance in esterification. *Microporous Mesoporous Mater.* **2014**, *186*, 155–162.
- (16) De Gregorio, G. F.; Prado, R.; Vriamont, C.; Erdocia, X.; Labidi, J.; Hallett, J. P.; Welton, T. Oxidative depolymerization of lignin using a novel polyoxometalate-protic ionic liquid system. *ACS Sustainable Chem. Eng.* **2016**, *4*, 6031–6036.
- (17) Li, H.; Chen, J.; Hua, L.; Qiao, Y.; Yu, Y.; Pan, Z.; Yang, H.; Hou, Zh. Polyoxometalate and copolymer-functionalized ionic liquid catalyst for esterification. *Pure Appl. Chem.* **2011**, *84*, S41–S51.
- (18) Zhang, W.; Leng, Y.; Zhao, P.; Wang, J.; Zhu, D.; Huang, J. Heteropolyacid salts of N-methyl-2-pyrrolidonium as highly efficient and reusable catalysts for prins reactions of styrenes with formalin. *Green Chem.* **2011**, *13*, 832–834.
- (19) Herrmann, S.; Kostrzewa, M.; Wierschem, A.; Streb, C. Polyoxometalate ionic liquids as self-repairing acid-resistant corrosion protection. *Angew. Chem., Int. Ed.* **2014**, *53*, 13596–13599.
- (20) Jiang, W.; Zheng, D.; Xun, S.; Qin, Y.; Lu, Q.; Zhu, W.; Li, H. Polyoxometalate-based ionic liquid supported on graphite carbon induced solvent-free ultra-deep oxidative desulfurization of model fuels. *Fuel* **2017**, *190*, 1–9.
- (21) Xu, L.; Wang, Y.; Yang, X.; Yu, X.; Guo, Y.; Clark, J. H. Preparation of mesoporous polyoxometalate-tantalum pentoxide composite catalyst and its application for biodiesel production by esterification and transesterification. *Green Chem.* **2008**, *10*, 746–755.
- (22) Ghasemi, M. H.; Kowsari, E. Convenient N-alkylation of amines using an effective magnetically separable supported ionic liquid containing an anionic polyoxometalate. *Res. Chem. Intermed.* **2017**, *43*, 1957–1968.
- (23) Ozdokur, K. V.; Moniruzzaman, M.; Yanik, J.; Ono, T. Synthesis and characterization of a polyoxometalate-based ionic liquid catalyst for delignification of wood biomass. *Wood Sci. Technol.* **2016**, *50*, 1213–1226.
- (24) Moosawi-Zare, A. R.; Leclerclaronze, N.; Floquet, S.; Abramov, P. A.; Sokolov, M. N.; Cordier, S.; Ponchel, A.; Monflier, E.; Bricout, H.; Landy, D.; Haouas, M.; Marrot, J.; Cadot, E. Polyoxometalate, cationic cluster and  $\gamma$ -cyclodextrin: from primary interactions to supramolecular hybrid materials. *J. Am. Chem. Soc.* **2017**, *139*, 12793–12803.
- (25) Moosavi-Zare, A. R.; Zolfigol, M. A.; Khakyzadeh, V.; Böttcher, C.; Beyzavi, M. H.; Zare, A.; Hasaninejad, A.; Luque, R. Facile preparation of a nanostructured functionalized catalytically active organosalt. *J. Mater. Chem. A* **2014**, *2*, 770–777.
- (26) Zhao, P.; Zhang, M.; Wu, Y.; Wang, J. Heterogeneous selective oxidation of sulfides with H<sub>2</sub>O<sub>2</sub> catalyzed by ionic liquid-based polyoxometalate salts. *Ind. Eng. Chem. Res.* **2012**, *51*, 6641–6647.
- (27) Liu, F.; Zheng, A.; Noshadi, I.; Xiao, F. S. Design and synthesis of hydrophobic and stable mesoporous polymeric solid acid with ultra strong acid strength and excellent catalytic activities for biomass transformation. *Appl. Catal., B* **2013**, *136–137*, 193–201.
- (28) Liu, F.; Kamat, R. K.; Noshadi, I.; Peck, D.; Parnas, R. S.; Zheng, A.; Qi, C.; Lin, Y. Depolymerization of crystalline cellulose catalyzed by acidic ionic liquids grafted onto sponge-like nanoporous polymers. *Chem. Commun.* **2013**, *49*, 8456–8458.
- (29) Li, J.; Li, D.; Xie, J.; Liu, Y.; Guo, Z.; Wang, Q.; Lyu, Y.; Zhou, Y.; Wang, J. Pyrazinium polyoxometalate tetrakaidecahedron-like crystals esterify oleic acid with equimolar methanol at room temperature. *J. Catal.* **2016**, *339*, 123–134.
- (30) Zheng, A.; Zhang, H.; Lu, X.; Liu, S. B.; Deng, F. Theoretical predictions of <sup>31</sup>P NMR chemical shift threshold of trimethylphosphine oxide adsorbed on solid acid catalysts. *J. Phys. Chem. B* **2008**, *112*, 4496–4505.
- (31) Feng, N.; Zheng, A.; Huang, S. J.; Zhang, H.; Yu, N.; Yang, C. Y.; Liu, S. B.; Deng, F. Combined solid-state NMR and theoretical calculation studies of brønsted acid properties in anhydrous 12-molybdophosphoric acid. *J. Phys. Chem. C* **2010**, *114*, 15464–15472.
- (32) Han, X. X.; He, Y. F.; Hung, C. T.; Liu, L. L.; Huang, S. J.; Liu, S. B. Efficient and reusable polyoxometalate-based sulfonated ionic liquid catalysts for palmitic acid esterification to biodiesel. *Chem. Eng. Sci.* **2013**, *104*, 64–72.
- (33) Zhang, J.; Xie, B.; Wang, L.; Yi, X.; Wang, C.; Wang, G.; Dai, Z.; Zheng, A.; Xiao, F. S. Zirconium oxide supported palladium nanoparticles as a highly efficient catalyst in the hydrogenation–

amination of levulinic acid to pyrrolidones. *ChemCatChem* **2017**, *9*, 2661–2667.

(34) Li, J.; Li, S.; Zheng, A.; Liu, X.; Yu, N.; Deng, F. Solid-state NMR studies of host-guest interaction between UiO-67 and light alkane at room temperature. *J. Phys. Chem. C* **2017**, *121*, 14261–14268.

(35) Zhao, H.; Zeng, L.; Li, Y.; Liu, C.; Hou, B.; Wu, D.; Feng, N.; Zheng, A.; Xie, X.; Su, S.; et al. Polyoxometalate-based ionic complexes immobilized in mesoporous silicas prepared via a one-pot procedure: Efficient and reusable catalysts for H<sub>2</sub>O<sub>2</sub>-mediated alcohol oxidations in aqueous media. *Microporous Mesoporous Mater.* **2013**, *172*, 67–76.

(36) Satasia, S. P.; Kalaria, P. N.; Raval, D. K. Heteropolyanion-based sulfated ionic liquid catalyzed formamides synthesis by grindstone chemistry. *J. Mol. Catal. A: Chem.* **2014**, *391*, 41–47.

(37) Liu, F.; Kong, W.; Wang, L.; Yi, X.; Noshadi, I.; Zheng, A.; Qi, C. Efficient biomass transformations catalyzed by graphene-like nanoporous carbons functionalized with strong acid ionic liquids and sulfonic group. *Green Chem.* **2015**, *17*, 480–489.

(38) Liu, F.; Zuo, S.; Kong, W.; Qi, C. High-temperature synthesis of strong acidic ionic liquids functionalized, ordered and stable mesoporous polymers with excellent catalytic activities. *Green Chem.* **2012**, *14*, 1342–1349.

(39) Liu, F.; Wang, L.; Sun, Q.; Zhu, L.; Meng, X.; Xiao, F. S. Transesterification catalyzed by ionic liquids on superhydrophobic mesoporous polymers: heterogeneous catalysts that are faster than homogeneous catalysts. *J. Am. Chem. Soc.* **2012**, *134*, 16948.

(40) Xu, S.; Zhou, P.; Zhang, Z.; Yang, C.; Zhang, B.; Deng, K.; Bottle, S.; Zhu, H. Selective oxidation of 5-hydroxymethylfurfural to 2,5-furandicarboxylic acid using O<sub>2</sub> and a photocatalyst of Co-thioporphyrazine bonded to g-C<sub>3</sub>N<sub>4</sub>. *J. Am. Chem. Soc.* **2017**, *139*, 14775.

(41) Wang, J.; Zhang, Z.; Jin, S.; Shen, X. Efficient conversion of carbohydrates into 5-hydroxymethylfurfural and 5-ethoxymethylfurfural over sulfonic acid-functionalized mesoporous carbon catalyst. *Fuel* **2017**, *192*, 102.